Supplemental Material for "Emergent SU(3) symmetry in random spin-1 chains"

V. L. Quito,[1] José A. Hoyos,[2] and E. Miranda[1]

[1] *Instituto de Física Gleb Wataghin, Unicamp, Rua Sérgio Buarque de Holanda, 777, CEP 13083-859 Campinas, SP, Brazil*
[2] *Instituto de Física de São Carlos, Universidade de São Paulo, C.P. 369, São Carlos, SP 13560-970, Brazil*

(Dated: December 15, 2014)

THE SU(3)-SYMMETRIC POINTS

We first write out in detail the 8 generators of the SU(3) group in the defining (quark) representation in terms of the spin-1 operators. The Cartesian vector and symmetric rank-2 tensor operators, S_μ and $T_{\mu\nu} = S_\mu S_\nu + S_\nu S_\mu$ $(\mu, \nu = x, y, z)$, form a complete basis set of 9 elements spanning the space of 3×3 Hermitian matrices. The generators we seek are the complete set of 8 *traceless* Hermitian matrices. A convenient choice is

$$\Lambda_1 = S_x, \tag{1}$$
$$\Lambda_2 = S_y, \tag{2}$$
$$\Lambda_3 = S_z, \tag{3}$$
$$\Lambda_4 = S_x S_y + S_y S_x, \tag{4}$$
$$\Lambda_5 = S_x S_z + S_z S_x, \tag{5}$$
$$\Lambda_6 = S_y S_z + S_z S_y, \tag{6}$$
$$\Lambda_7 = S_x^2 - S_y^2, \tag{7}$$
$$\Lambda_8 = \frac{1}{\sqrt{3}}\left(2S_z^2 - S_x^2 - S_y^2\right). \tag{8}$$

In terms of these generators, the linear Heisenberg term is obvious, whereas the bilinear term can be written as

$$\left(\mathbf{S}\cdot\mathbf{S}'\right)^2 = \frac{4}{3} - \frac{1}{2}\sum_{a=1}^{3}\Lambda_a\Lambda'_a + \frac{1}{2}\sum_{a=4}^{8}\Lambda_a\Lambda'_a. \tag{9}$$

The generic Hamiltonian for two adjacent sites in terms of θ $(\tan\theta = D/J)$ is

$$H(\theta) = \cos\theta\mathbf{S}\cdot\mathbf{S}' + \sin\theta\left(\mathbf{S}\cdot\mathbf{S}'\right)^2 \tag{10}$$
$$= \frac{4}{3}\sin\theta + \left(\cos\theta - \frac{1}{2}\sin\theta\right)\sum_{a=1}^{3}\Lambda_a\Lambda'_a \tag{11}$$
$$+\frac{1}{2}\sin\theta\sum_{a=4}^{8}\Lambda_a\Lambda'_a. \tag{12}$$

The point $\theta = \frac{\pi}{4}$ then becomes

$$H\left(\theta = \frac{\pi}{4}\right) \propto \mathbf{S}\cdot\mathbf{S}' + \left(\mathbf{S}\cdot\mathbf{S}'\right)^2 \tag{13}$$
$$= \frac{4}{3} + \frac{1}{2}\sum_{a=1}^{8}\Lambda_a\Lambda'_a, \tag{14}$$

whose SU(3) invariance is manifest. The other SU(3)-invariant point at $\theta = -\frac{\pi}{2}$ is

$$H\left(\theta = -\frac{\pi}{2}\right) = -\left(\mathbf{S}\cdot\mathbf{S}'\right)^2 \tag{15}$$
$$= -\frac{4}{3} + \frac{1}{2}\sum_{a=1}^{3}\Lambda_a\Lambda'_a - \frac{1}{2}\sum_{a=4}^{8}\Lambda_a\Lambda'_a. \tag{16}$$

In order to make the SU(3) invariance manifest in this case, we must first realize that the antiquark representation, the complex conjugate of the quark one, is obtained by applying the following operation to the generator matrices

$$\left(\Lambda_a\right)_{ij} \to -\left(\Lambda_a\right)^*_{ij}. \tag{17}$$

We get (assuming the usual basis of eigenvectors of S_z)

$$\Lambda_1 \to -S_x, \tag{18}$$
$$\Lambda_2 \to S_y, \tag{19}$$
$$\Lambda_3 \to -S_z, \tag{20}$$
$$\Lambda_4 \to S_x S_y + S_y S_x, \tag{21}$$
$$\Lambda_5 \to -S_x S_z - S_z S_x, \tag{22}$$
$$\Lambda_6 \to S_y S_z + S_z S_y, \tag{23}$$
$$\Lambda_7 \to -S_x^2 + S_y^2, \tag{24}$$
$$\Lambda_8 \to -\frac{1}{\sqrt{3}}\left(2S_z^2 - S_x^2 - S_y^2\right). \tag{25}$$

An equivalent representation to Eqs. (18)-(25) is obtained if we make a rotation of π around the y-axis: $S_x \to -S_x$, $S_z \to -S_z$. After these transformations, we find, denoting the antiquark representation by a tilde,

$$\tilde{\Lambda}_a = \Lambda_a \ (a = 1, 2, 3), \tag{26}$$
$$\tilde{\Lambda}_a = -\Lambda_a \ (a = 4, 5, 6, 7, 8). \tag{27}$$

From Eqs. (16) and (26)-(27), we see that the $\theta = -\frac{\pi}{2}$ point couples sites belonging to the quark and the antiquark representations

$$H\left(\theta = -\frac{\pi}{2}\right) = -\frac{4}{3} + \frac{1}{2}\sum_{a=1}^{8}\Lambda_a\tilde{\Lambda}'_a. \tag{28}$$

Note that the FM points $\theta = -\frac{3\pi}{4}$ and $\theta = \frac{\pi}{2}$ also display global SU(3) invariance since

$$H\left(\theta = \frac{\pi}{2}\right) = -H\left(\theta = -\frac{\pi}{2}\right), \tag{29}$$
$$H\left(\theta = \frac{3\pi}{4}\right) = -H\left(\theta = \frac{\pi}{4}\right). \tag{30}$$

NUMERICAL RESULTS

We have implemented the full SDRG procedure described in the main text numerically in order to check our findings. We have first focused on initial Hamiltonians in which all bonds have the same $\theta_i = \theta_0$ with $-\frac{3\pi}{4} < \theta_0 < \frac{\pi}{2}$, while J is uniformly distributed in the interval $0 \leq J \leq 1$. The results were obtained for chain lengths of $L_0 \sim 10^6$ spins, averaged over 20 realizations of disorder. We have verified that, although initially the θ distribution broadens, *asymptotically all θ_i tend to unique values.*

In Fig. 1, we show, for some representative cases, the average value of $\tan\theta$ as the mean distance L between undecimated spin clusters is increased. The latter is given by $L = \frac{L_0}{N}$, where N is the number of undecimated spin clusters. For $-\frac{\pi}{2} < \theta_0 < \frac{\pi}{4}$ (three blue lowest curves), the flow is towards (FP1), with $\theta = 0$. When $-\frac{3\pi}{4} < \theta_0 < -\frac{\pi}{2}$ (red, topmost curve), the flow tends to (FP2), with $\tan\theta = 2$, $D < 0$. The green (2nd and 3rd from the top) curves correspond to the interval $\frac{\pi}{4} < \theta_0 < \frac{\pi}{2}$, for which the systems flows to (FP3), $\tan\theta = 2$, $D \lessgtr 0$ with equal probability. For the specific case of $\theta_0 = \frac{\pi}{4}$ (black curve with down triangles), we plotted instead the inverse of $\langle\cot\theta\rangle$ on the right-hand vertical axis. This corresponds to flows at the unstable (FP8), for which asymptotically half the bonds have $\theta = -\frac{\pi}{2}$ and half $\theta = \frac{\pi}{4}$, such that $\langle\cot\theta\rangle \to 1/2$. These plots confirm the delineation of the fixed points and basins of attraction described in the main text.

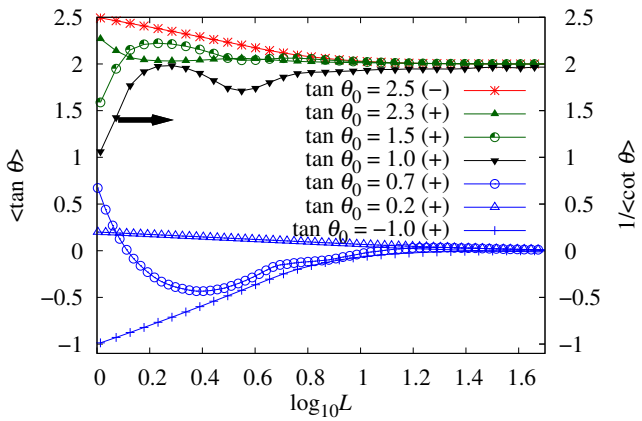

Figure 1. (Color online) Some representative SDRG flows: mean value of $\langle\tan\theta\rangle$ as a function of the average distance L between undecimated spin clusters, for different values of the angle θ_0 of the initial distribution. The sign in parentheses is the sign of J's in the initial distribution. For $\tan\theta_0 = 1$, we plot $\frac{1}{\langle\cot\theta\rangle}$ on the right-hand vertical axis instead.

Although the flow in the region $(-\frac{\pi}{2} < \theta_0 < \frac{\pi}{4})$ is characterized by the disappearance of the biquadratic couplings, there is a clear difference in the transient SDRG flow between the cases $\arctan\frac{1}{3} < \theta_0 < \frac{\pi}{4}$ and $-\frac{\pi}{2} < \theta_0 < \arctan\frac{1}{3}$. The latter only involves singlet-forming decimations [see Eq. (2) and Fig. 2 of the main text]. As a result, $\langle\tan\theta\rangle$ flows monotonically to 0 ($\tan\theta_0 = 0.2$ and -1 in Fig. 1). When $\arctan\frac{1}{3} < \theta_0 < \frac{\pi}{4}$, however, both types of decimations rules occur [Eqs. (2) and (3) of the main text], necessarily generating negative angles, in such a way that $\langle\tan\theta\rangle$ may change sign in the course of the flow ($\tan\theta_0 = 0.7$ in Fig. 1).

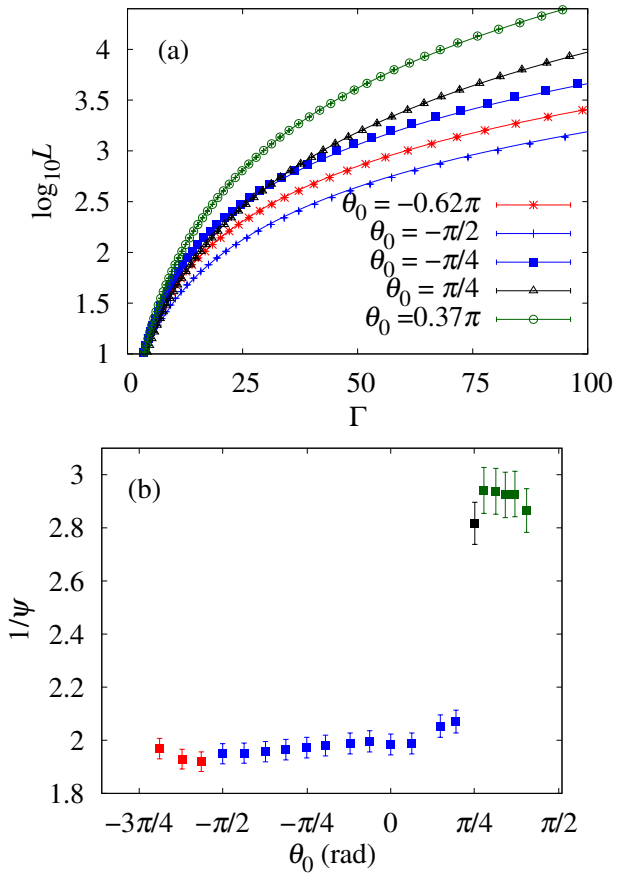

Figure 2. (Color online) Numerical determination of the ψ exponent: (a) mean distance L between undecimated spin clusters as a function of $\Gamma = \ln\frac{\Omega_0}{\Omega}$, where Ω is the renormalization group energy scale. The full lines are fits to Eq. (31); (b) reciprocal of the activated dynamical scaling exponent ψ as a function of initial angle θ_0.

In order to numerically determine the value of ψ in each of the RSPs of the phase diagram, we tracked the dependence of the cutoff energy scale $\Gamma \equiv \ln\frac{\Omega_0}{\Omega}$ (where Ω_0 is the largest initial Δ_i) on the average distance between undecimated spin clusters L. In Fig. 2(a) we show the results for several initial angles θ_0. We have fitted our data to the form

$$\log_{10} L = a + \frac{1}{\psi}\log_{10}(1 + b\Gamma)\,, \qquad (31)$$

where a, b and $\frac{1}{\psi}$ are fitting parameters. As seen in Fig. 2(a), it fits remarkably well the numerical data. For $b\Gamma \gg 1$, we recover the more familiar activated dynamical scaling form $L \sim \Gamma^{\frac{1}{\psi}}$. The numerically determined values of ψ can be seen in Fig. 2(b) as a function of θ_0. There is good agreement with the predicted exponents of the mesonic ($\psi_M = \frac{1}{2}$) and baryonic ($\psi_B = \frac{1}{3}$) RSPs and a sharp jump at the border between them ($\theta_0 = \frac{\pi}{4}$) can be clearly seen. The error bars were estimated from the uncertainty in the range over which Eq. 31 is valid.

BEHAVIOR AT WEAK DISORDER

The spontaneously dimerized phase ($-\frac{3\pi}{4} < \theta < -\frac{\pi}{4}$) is unstable against weak disorder due to the formation of weakly coupled domain walls [1, 2]. Weak disorder can also be shown to be a relevant perturbation at the SU(3)-symmetric point $\theta = \frac{\pi}{4}$ [3]. In general, we expect disorder to be perturbatively relevant in the entire gapless phase $\frac{\pi}{4} \leq \theta \leq \frac{\pi}{2}$.

Infinitesimally weak disorder is an irrelevant perturbation in the gapped Haldane phase ($-\frac{\pi}{4} < \theta < \frac{\pi}{4}$). The behavior was determined in detail at $\theta_i = 0$ [2, 4–7]. Gradually increasing the disorder at this point eventually leads to the closure of the Haldane gap (although the topological order parameter initially retains a finite value [8]) and to the emergence of a quantum Griffiths region [9] with conventional power-law scaling $\Omega \sim L^{-z}$. In this region, the spin correlations are short ranged, the magnetic susceptibility $\chi \sim T^{1/z-1}$, and the specific heat $c \sim T^{1/z}$. The dynamical exponent z is disorder-dependent and diverges at a critical point [4–7, 9, 10]. Above this critical disorder value, the system enters a universal RSP governed by an IRFP with $\psi = \frac{1}{2}$. This generic behavior is expected to hold throughout the region $-\frac{\pi}{4} < \theta < \frac{\pi}{4}$, with the exception of the AKLT point.

At the AKLT point ($\theta = \arctan\frac{1}{3}$), the ground state is exactly known [11]. Provided the local angle θ_i is everywhere equal to $\arctan\frac{1}{3}$, the ground state will be disorder independent [12]. We note that this is reflected in the SDRG procedure by the closure of the gap of a spin pair $\Delta_i = 3J_i\left|\tan\theta_i - \frac{1}{3}\right|$, which makes it ill-defined in the vicinity of the AKLT point. The Haldane gap, however, will vanish in the strong-disorder limit when the distribution of coupling constants is not bounded from below.

Although tailored to be accurate only in the strong disorder regime, the SDRG flow has been shown to break down whenever weak disorder is irrelevant [2, 4–7, 9, 13]. This is signaled by the fact that the coupling constant distributions do not broaden as the energy scale is reduced. We only detect this break-down in the topological phase $-\frac{\pi}{4} < \theta < \frac{\pi}{4}$ [14]. In fact, our numerics indicate that weak disorder may possibly be relevant even inside the Haldane phase near the edges $\pm\frac{\pi}{4}$. Since the dimerized ($-\frac{3\pi}{4} < \theta < -\frac{\pi}{4}$) and the gapless ($\frac{\pi}{4} < \theta < \frac{\pi}{2}$) phases are expected to be destabilized by any amount of disorder and we have not found any other fixed point numerically, we conjecture that no other phase transition happens at intermediate disorder strength. We thus obtain the weak disorder region of the phase diagram sketched in Fig. 1 of the main text.

[1] K. Yang, R. A. Hyman, R. N. Bhatt, and S. M. Girvin, J. Appl. Phys. **79**, 5096 (1996).
[2] B. Boechat, A. Saguia, and M. A. Continentino, Solid State Commun. **98**, 411 (1996).
[3] R. G. Pereira, Private communication.
[4] R. A. Hyman and K. Yang, Phys. Rev. Lett. **78**, 1783 (1997).
[5] C. Monthus, O. Golinelli, and T. Jolicoeur, Phys. Rev. Lett. **79**, 3254 (1997).
[6] C. Monthus, O. Golinelli, and Th. Jolicoeur, Phys. Rev. B **58**, 805 (1998).
[7] A. Saguia, B. Boechat, and M. A. Continentino, Phys. Rev. Lett. **89**, 117202 (2002).
[8] R. A. Hyman, K. Yang, R. N. Bhatt, and S. M. Girvin, Phys. Rev. Lett. **76**, 839 (1996).
[9] K. Damle, Phys. Rev. B **66**, 104425 (2002).
[10] S. Bergkvist, P. Henelius, and A. Rosengren, Phys. Rev. B **66**, 134407 (2002).
[11] I. Affleck, T. Kennedy, E. H. Lieb, and H. Tasaki, Phys. Rev. Lett. **59**, 799 (1987).
[12] X. Chen, Z.-C. Gu, Z.-X. Liu, and X.-G. Wen, Science **338**, 6114 (2012).
[13] J. A. Hoyos, Phys. Rev. E **78**, 032101 (2008).
[14] In this case, it is still possible to use the SDRG through an appropriate generalization of the recursion relations as in reference [5].